Control design of a gyro-based wave energy converter for autonomous underwater vehicle

IOP Conf. Series: Materials Science and Engineering **563** (2019) 042073 doi:10.1088/1757-899X/563/4/042073

Control design of a gyro-based wave energy converter for autonomous underwater vehicle

Puyue Hou[1], Li Liu[1], Liming Guo[1], Yuying Zhou[2]

[1]School of Automation Science and Electrical Engeering,Beihang University,China

[2]Systems Engineering Research Institute

Corrosponding author's e-mail address: liulibh@163.com

Abstract. Autonomous Underwater Vehicle (AUV) is an intelligent machine that works at hazardous underwater environment. It can only operate for hours or days at a time by battery charging system. This paper presents a new gyroscopic charging system to reform the traditional way. The new system utilizes the gyroscopic effects of a large rotating flywheel in combination with a controlled power take-off device to extract power from wave motion. In this paper, a gyroscopic energy converter model is given, which contains a description of dynamic equation and controlling design. Consequently, a detailed process of applying the gyroscopic system to a typical AUV is shown. The gyroscopic charging system promises to reduce AUV battery requirements negating the necessity to carry sufficient energy reserves (size and weight) for entire missions, reduce costs by freeing support vessel time (a major cost component in AUV deployment) and enable AUVs to be remotely and renewably recharged at sea, indefinitely extending missions. Software simulation is the main method to prove the validation of the results. The results show that the generated power is sufficient to provide power for AUV which is better than the battery charging system.

1. Introduction

Ocean wave energy is a highly energetic source that is considered as one of the most promising renewable source. It is reported that the ocean contains about 2TW which is in the magnitude of the world's yearly power demand[1]. Besides, the wave energy density is around 2–3 kW/ m^2 over an area perpendicular to the wave propagation[2]. When compared with the power demands and typical dimensions of Autonomous/Unmanned Underwater Vehicles (AUVs or UUVs), see Table 1, the available ambient power is significant and may provide a means to sustain these vehicles remotely, renewably and indefinitely[3].

The traditional charging way for AUV mainly includes battery charging and solar powered system. The former uses battery as driving power. Zinc-silver battery and lithium battery are the most commonly used batteries, which has already been applied to many AUVs or UUVs, such as STDV, AUSS, Bluefin-21[4]. Batteries has the advantage of high energy density and stable duration performance, but it provides definite power which constrains AUV's task time. The average duration of AUV is only about 25 hours. Furthermore, it also has safety problem and becomes a big burden for AUV (generally 20% of AUV mass).The later involves several solar powered AUVs and solar assisted commercial ASVs systems e.g., SAUV-II, Autonaut, WaveGlider and C-Enduro. While solar potentially offers unlimited mission durations, it is limited to night-time missions and daylight recharging strategies and is susceptible to bio fouling [5].

Table 1. Summary of various torpedo style AUV power demand

Vehicle	Mass (kg)	Length (L) (m)	Diameter (D) (cm)	Energy (kWh)	Endurance (h)	Power (P) (W)	Power per area (P/LD) (kW/m2)
Iver2-580-S	20.5	1.52	14.7	0.6	14	43	0.19
Folaga AUV	31.0	2.04	16.0	0.5	6	90	0.28
REMUS 100-S	38.5	1.60	19.0	1.0	10	100	0.33
REMUS 600	240.0	3.25	32.4	5.2	70	74	0.07
Bluefin 12D	260.0	4.32	32.0	7.5	30	250	0.18
Dorado class AUV	680.0	5.30	53.0	11.0	17.5	629	0.22
Bluefin 21	750.0	4.93	53.0	13.5	25	540	0.21
Abyss AUV	880.0	4.00	66.0	11.2	24	467	0.18
REMUS 6000	884.0	3.84	71.0	11.8	22	536	0.2
Eagle ray AUV	940.0	4.60	69.0	29.4	30	979	0.31
Echo surveyor IV	1450.0	5.40	100.0	45.0	50	900	0.17

In this paper, the author proposes a new charging system that utilizes wave energy to motivate AUV, which is called gyroscopic wave energy converter. The new recharging system uses a gyroscope to create an internal inertial reaction able to harvest wave power without exposing mechanical parts to the harsh oceanic environment. The gyroscope drives a PTO system (Power Take Off) converting mechanical power into electrical power. It's not the first time that this type of wave energy converter is proposed. Townsend N and Shenoi A (2014) firstly proposed a complete solution to apply a gyro-based wave converter to AUV, including dynamic equation and extracted power analysis[6]. Consequently, a theoretical description of the system and simulation results for a range of geometrically scaled torpedo style AUVs are presented by the same author[7]. However, neither of them ensures the correctness of the fundamental physical model, which makes the result unconvincing. In this paper, the author will revise the gyroscopic formula and obtain the non-linear AUV dynamic equation, then use the commercial software to check the formula. There are mainly four sections in the paper: in the next section, the mathematical model of gyroscopic system in time domain is defined. In the third section, an AUV dynamic model is given both in time and frequency domain, including the parameter identification from the frequency dependent hydrodynamic data. A series of explicit results of the hull system, obtained in Simulink, will be checked with reliable data computed by the hydrodynamic software AWQA. In the fourth section the author firstly designs the gyroscopic size to match the AUV, then outlines the method of controlling the PTO to maximize the power extracted from gyroscope, finally comparing it with power that AUV sensors need to see if the gyro charging system meet the demand of AUV .Conclusions are drawn in section five.

2. Mechanical equation of gyroscopic system

Figure 1 shows the skeleton of the whole system. The left-hand picture represents a typical torpedo style AUV, with a cylindrical body and hemispherical nose and tail sections, while the right-hand picture that concludes the flywheel, gimbal and PTO represents the gyroscopic system. To describe the system, three reference framework must be introduced: Inertial coordinate system (X, Y, Z), hull-fixed coordinate system (x_b, y_b, z_b) and gyroscope structure-fixed coordinate system (x, y, z). The following derivation is based on two assumptions: firstly, the x_b-axis is oriented towards the bow and coincides with the sea wave direction. Secondly, the flywheel rotates at a constant speed about y-axis. As the result, the hull generates pitch motion β about the y_b-axis due to the induced wave motion. Consequently, the interaction between the rotating flywheel and pitch motion generates a gyroscopic torque around the z-axis, which can be exploited by PTO to generate electrical power.

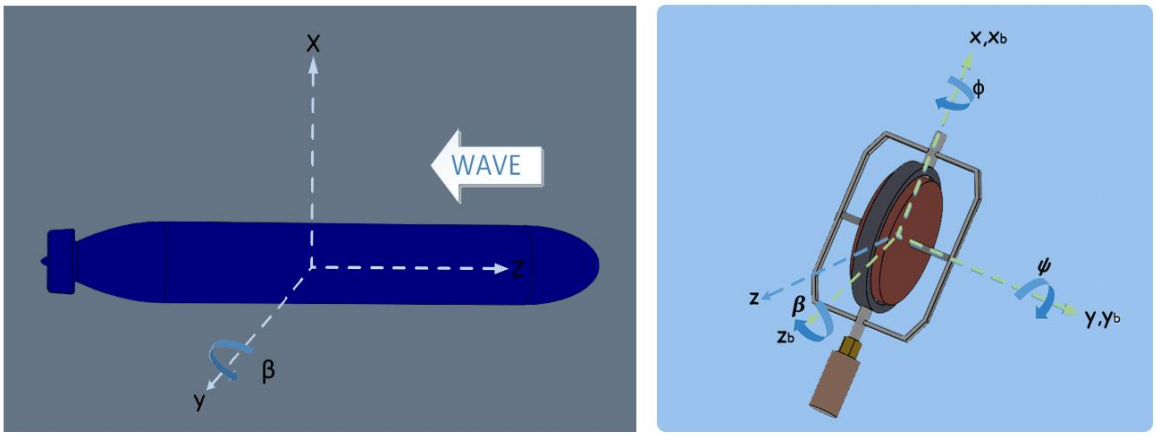

Figure 1. Gyroscopic system schematic and coordinate frame definitions

We denote the precession angle from (x,y,z) to (x_b,y_b,z_b) by $(0,0,\varphi)$, and the AUV roll, pitch and yaw angle from (x_b,y_b,z_b) to (X,Y,Z) by (α,β,γ). In this paper only pitch motion is considered. The flywheel rotating angle about y-axis is defined as ψ.

Following the rotate transformation principle, the relative rotation angular speed from flywheel to (X,Y,Z) is defined:

$$\Omega_f = \begin{bmatrix} \cos\varphi & \sin\varphi & 1 \\ -\sin\varphi & \cos\varphi & 0 \\ 0 & 0 & 1 \end{bmatrix} \begin{bmatrix} \dot{\beta} \\ 0 \\ 0 \end{bmatrix} + \begin{bmatrix} 0 \\ \dot{\psi} \\ 0 \end{bmatrix} + \begin{bmatrix} 0 \\ 0 \\ \dot{\varphi} \end{bmatrix} = \begin{bmatrix} \dot{\beta}\cos\varphi \\ \dot{\psi} - \dot{\beta}\sin\varphi \\ \dot{\varphi} \end{bmatrix} \tag{1}$$

Considering flywheel speed is much greater than wave induced pitch angular speed, Eq.(1) could be simplified as below:

$$\Omega_f = \begin{bmatrix} \dot{\beta}\cos\varphi \\ \dot{\psi} \\ \dot{\varphi} \end{bmatrix} \tag{2}$$

The moment of momentum of flywheel:

$$H_f = I_f \Omega_f = \begin{bmatrix} I_x & 0 & 0 \\ 0 & I_y & 0 \\ 0 & 0 & I_z \end{bmatrix} \Omega_f = \begin{bmatrix} I_x\dot{\beta}\cos\varphi \\ I_y\dot{\psi} \\ I_z\dot{\varphi} \end{bmatrix} \tag{3}$$

Following the principle that $\mathbf{M} = \frac{d\mathbf{H}}{dt} + \boldsymbol{\Omega} \times \mathbf{H}$, The gyroscopic moments about (x,y,z) is derived:

$$M_g = \begin{bmatrix} I_x\ddot{\beta}\cos\varphi - I_x\dot{\beta}\sin\varphi + \left(I_z\dot{\beta}\sin\varphi + I_y\dot{\psi}\right)\dot{\varphi} \\ I_y\ddot{\psi} - I_x\dot{\beta}\dot{\varphi}\cos\varphi + I_z\dot{\beta}\dot{\varphi}\cos\varphi \\ I_z\ddot{\varphi} - I_y\dot{\psi}\dot{\beta}\cos\varphi - I_x\dot{\beta}^2\cos\varphi\sin\varphi \end{bmatrix} \tag{4}$$

Therefore, the moment about the precession axis could be expressed as:

$$I_z\ddot{\varphi} - I_y\dot{\psi}\dot{\beta}\cos\varphi - I_x\dot{\beta}^2\cos\varphi\sin\varphi = T_z \tag{5}$$

Where T_z represents the PTO feedback torque.

Considering the strong coupling of Eq.(5), it is normally simplified by neglecting its second term as it is two orders of magnitude smaller than the others :

$$I_Z \ddot{\varphi} - I_Y \dot{\psi}\dot{\beta}\cos\varphi = T_Z \tag{6}$$

3. Hydrodynamics model of AUV

3.1. Hydrodynamics equation of the AUV

The hydrodynamic equation can be expressed as:

$$(\mathbf{M} + \mathbf{A}_\infty)\ddot{\zeta} + \int_0^t \mathbf{K}(t - t')\dot{\zeta}(t')dt' + \mathbf{G}\zeta = \tau_{exc} \tag{7}$$

It is a matrix-form formula, which contains the forces and moments in the six degree of freedom. The displacement vector $\zeta = [x, y, z, \alpha, \beta, \gamma]$ defines the position (x -surge, y -sway, z -heave) and Euler angles (α -roll, β -pitch, γ -yaw). M represents the AUV generalized mass. The parameter $\mathbf{A_\infty}$ is a constant positive-definite matrix, in which the entries are the added mass coefficients. The convolution term is known as a fluid-memory model, part of the radiation force $\boldsymbol{\tau}_{\mathbf{rad}}$. The kernel of the convolution term, $\mathbf{K}(\mathbf{t})$, is called retardation or memory impulse responses function. $\mathbf{G}$ is the restoring coefficient that is related to the distance between gravity center and metacenter of AUV[8].

Eq.(7) is generally known as *Cummins Equation*[9]. Due to the non-linearity of the convolution term and difficulty of obtaining $K(t)$ data in time domain, it's hard to solve Eq.(4) both in analytic and numerical way. An alternative way is to solve the convolution problem in frequency domain.

The frequency-domain form of $\boldsymbol{\tau}_{\mathbf{rad}}$ can be expressed as below[10]:

$$\boldsymbol{\tau}_{rad}(jw) = w^2\mathbf{A}(w)\zeta(jw) - jw\mathbf{B}(w)\zeta(jw) \tag{8}$$

$A(w)$ and $B(w)$ represents the frequency-dependent added mass and potential damping, respectively. Eq.(7) in the frequency domain:

$$\left[-w^2[\mathbf{M} + \mathbf{A}(w)] + jw\mathbf{B}(w) + \mathbf{G}\right]\zeta(jw) = \boldsymbol{\tau}_{exc}(jw) \tag{9}$$

By using Laplace transform to Eq.(7), the transfer function of the system is shown:

$$\left[(\mathbf{M} + \mathbf{A}_\infty)s^2 + \mathbf{K}(s)s + \mathbf{G}\right]\zeta(s) = \boldsymbol{\tau}_{exc}(s) \tag{10}$$

Comparing (9) with (10), we can learn a relationship between $\mathbf{K}(\mathbf{jw})$ and $\mathbf{A}(\mathbf{w}), \mathbf{B}(\mathbf{w})$:

$$\mathbf{K}(jw) = \mathbf{B}(w) + jw(\mathbf{A}(w) - \mathbf{A}_\infty) \tag{11}$$

Where $\mathbf{A}_\infty$ following the definition: $A_\infty = \lim_{w\to\infty} A(w)$. As $\mathbf{A}(\mathbf{w})$ and $\mathbf{B}(\mathbf{w})$ could be obtained by the hydrodynamic software AWQA, a series data of $\mathbf{K}(\mathbf{jw})$ will be explicitly displayed. Once we obtain the whole coefficients of $K(s)$, the pitch motion could be presented by simulating Eq.(7) in MATLAB, readily integrated with the gyroscopic system. Unfortunately, AQWA only offers a set of finite frequency data of $\mathbf{A}(\mathbf{w})$ and $\mathbf{B}(\mathbf{w})$, therefore, it is of great necessity to do parametric identification of $\mathbf{K}(\mathbf{s})$.

3.2. Parametric identification of convolution model

Assuming the transfer function $k(s)$ (an element of matrix $\mathbf{K}(\mathbf{s})$ that represents the fluid-memory effect acting on a certain displacement or Euler angle) is formed as below:

$$k(s)=\frac{P(s)}{Q(s)}=\frac{p_r s^r+p_{r-1}s^{r-1}+\ldots+p_1 s+p_0}{s^n+q_{n-1}s^{n-1}+\ldots+q_0} \tag{12}$$

Table 2. Properties of retardation functions and implications on parametric approximations

Property	Implication on parametric models
(1) $\lim_{w\to o} K(jw)=0$	There are zero at s=0
(2) $\lim_{w\to\infty} K(jw)=0$	Strictly proper
(3) $\lim_{t\to o^+} K(t)\neq 0$	Relative degree 1
(4) $\lim_{t\to\infty} K(t)=0$	Input–output stable
(5)the mapping $\dot{\xi}\to\mu$ passive	K(jw) is positive real

The first step to do parametric identification is to set the constraints on $k(s)$ based on the priori information. As $k(t)$ represents the radiation force working on AUV, there are some properties of $k(s)$ possessed to coincide with the radiation potential property. Some of the literature has already derived the properties of $k(s)$, which are listed in table2[11].

The second step is to utilise the available information to identify the coefficients of $k(s)$. For a given set of finite-frequency data of $\mathbf{A}(\mathbf{w})$ and $\mathbf{B}(\mathbf{w})$, we could compute a group of non-parametric data $k(jw)$ by using Eq.(11).the LS method here is used to satisfy the accuracy of the approximation of the parametric transfer function $\hat{k}(s)$ with $k(jw)$ .Assuming the vector of the parameters $\theta=[p_r,\ldots,p_0,q_{n-1},\ldots q_1]$, the parameter estimation problem can be posed a complex LS curve fitting:

$$\theta^*=\underset{\theta}{\operatorname{argmin}}\sum_l w'_l\,\varepsilon_l^*\varepsilon_l \tag{13}$$

Where, the notion * indicates transpose complex conjugate, w'_l indicates weighting coefficients, and ε_l is defined as:

$$\varepsilon_l=k(jw_l)-\frac{P(jw_l,\theta)}{Q(jw_l,\theta)} \tag{14}$$

Eq.(13) is obviously a non-linear LS problem. It is general to linearize Eq.(13) for easier reckon:

$$\varepsilon'_l=Q(jw_l,\theta)k(jw_l)-P(jw_l,\theta) \tag{15}$$

Therefore, the non-linear LS problem is turned into a linear problem:

$$\boldsymbol{\theta}^*=\underset{\theta}{\operatorname{argmin}}\,\varepsilon'^{*}_l\,\mathbf{W}\varepsilon'_l \tag{16}$$

The problem with this linear formula can be solved by many mathematical tools. In MATLAB, there is a function called *invfreqs* for solving a typical LS problem.

There is a detail should be noticed when we apply the method into practice. How to set the weights in Eq.(16) remarkably influences the identification result. A constant weight matrix **W** would weight the fitting more heavily at high frequencies and less heavily at low frequencies .This weighting normally gives a bias in the parameter estimates leading to a worse result. Perez T, and Fossen T I (2011) proposes that setting the weighting matrix as a variable adjusted to the convergence velocity of θ^* that changes at each iteration[12]. The algorithm is summarised in the following:

1.Set $\mathbf{W}_0=\mathbf{I}$

2.Solve $\boldsymbol{\theta}_n^*=\underset{\theta}{\operatorname{argmin}}\,\varepsilon'^{*}_n\,\mathbf{W}_n\varepsilon'_n$

3. Set $\mathbf{W}_{n+1} = \mathrm{diag}\left(\left|Q\left(jw_n, \theta_n\right)\right|^{-2}\right)$ and repeating step 2 and 3.

In this paper, the author considers $k(s)$ in the degree of the pitch motion as the identification object. Due to the symmetry of AUV, we could decoupled the pitch motion from other degree of freedom. However, A_∞ is an unknown in step 2. One way is to use $A(w_{max})$ to substitute A_∞ for $\mathbf{A}(\mathbf{w})$ is a group of sequence with fast convergence, so it will not be a big difference between $A(w_{max})$ and A_∞. When applying it into practice, we find it doesn't work: the result shows $\hat{k}(s)$ contains poles of positive real part which means unstable. That is to say, $A(w_{max})$ of AUV is distant from A_∞. Another way is to extend the formula to avoid the problem caused by ignorant of A_∞. Eq.(8) can be alternatively expressed as:

$$\boldsymbol{\tau}_{rad} = \left[\frac{\mathbf{B}(jw)}{jw} + \mathbf{A}(jw)\right]\ddot{\zeta}(jw) \tag{17}$$

Eq.(9) offers another expression of radiation force:

$$\boldsymbol{\tau}_{rad}(s) = [\ A_\infty + \frac{P'(s)}{Q(s)}\ ]\ \ddot{\zeta}(s) \tag{18}$$

Where $P'(s) = sP(s)$.Comparing (17) to (18), we find it reasonable to identify transfer function $A_C(s)$ (defined as: $\mathbf{A_C}(\mathbf{jw}) = \frac{\mathbf{B}(\mathbf{jw})}{jw} + \mathbf{A}(\mathbf{jw})$) to be a transition function. Once we get the accurate coefficients of $A_C(s)$, we can definitely deduce the result of $\hat{k}(s)$ and A_∞.

Figure 2 and 3 show the identification result of a small displacement AUV under 2000kg. Figure 2 contains the identification result of $\mathbf{A_C}(\mathbf{s})$, with the comparing figure between $\mathbf{A}(\mathbf{w})$, $\mathbf{B}(\mathbf{w})$ and $\hat{\mathbf{A}}(\mathbf{w})$, $\hat{\mathbf{B}}(\mathbf{w})$.Figure 3 shows the identification result of $\hat{k}(s)$ and $\hat{k}(t)$, respectively. The identification result has a good approximation effect when the denominator degree reaches at 4, which is clearly demonstrated from the figure 2. $\hat{k}(s)$ is expressed as:

$$\hat{k}(s) = \frac{6.3731e04s^3 + 1.4265e05s^2 + 9.8207e04s}{s^4 + 8.1557s^3 + 26.2967s^2 + 51.6648s + 34.5994} \tag{19}$$

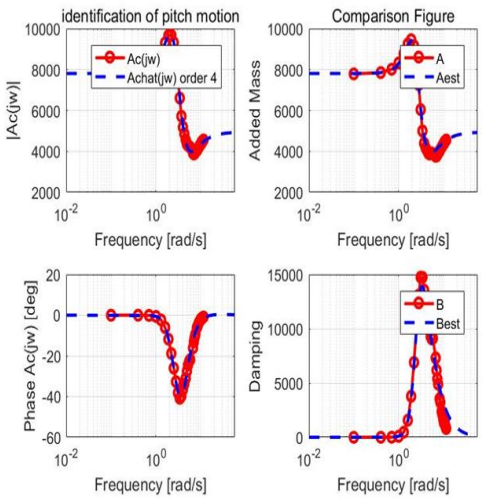

Figure 2. Identification results. Blue dotted lines represents the identified data, while red lines indicating the originated data

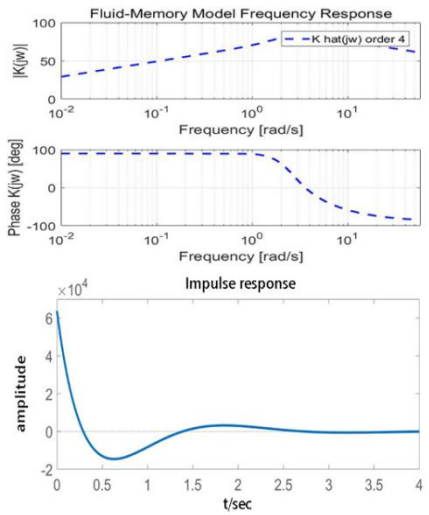

Figure 3. the image above is bode figure of $\hat{k}(s)$,and the image below is impulse response $\hat{k}(t)$

4. Control design to maximize extracted power

4.1. AUV pitch motion

A summary of AUV parameters are presented in Table 3. This is a typical torpedo style AUV, with a cylindrical body and hemispherical nose and tail sections, which is originated from AutoSUB and REMUS AUVs[13]. As we've got identification result from section 3, the pitch motion is simulated based on Eq.(10),that is shown in Figure 4. Added floating pitch motion RAO, the figure shows the simulation results is approximated successfully. τ_{exc} here is defined as regular sinusoidal wave excitation moment. The pitch motion under regular wave excitation oscillates around 0 degree, the maximum amplitude under 1m wave height doesn't exceed 30 degree, which means AUV could keep a relatively stable state under such ocean conditions.

Table 3. Simulation parameters

AUV particulars	Basis
Overall length (Lb) (m)	7
Diameter (m)	0.85
Longitudinal centre of gravity (from FP) (m)	3.5
Vertical centre of gravity (from AUV top, down) (m)	0.425
Displacement (kg)	1703
Mass moment of inertia (I55) (kgm2)	5418
Restoring coefficient (G)	176604
Gyroscopic system particulars	
Flywheel mass moment of inertia (Iy) (kgm2)	3.07
Flywheel mass moment of inertia (Ixx = Izz = Ig) (kgm2)	1.53
Flywheel tip velocity (constant) (m/s)	Up to 100
Initial precession (β, $\dot{\beta}$) (radians, rad/s)	(0,0)
Simulation parameters	
Time step (s)	0.01
Simulated time (s)	200

Wave Amplitude (ζ) (m)	1

4.2. Control design of gyroscopic system

To provide a reasonable flywheel dimension to assess the feasibility of the system, an optimised I-selection flywheel is selected[7]. A common design principle considers the flywheel mass had better not exceed 5% of AUV displacement. As a result, the flywheel mass is designed to be scaled to 4% of the AUV displacement is realistic. As battery mass normally accounts for 20% of total mass of AUV, the gyroscopic system takes large advantage at light loading. Table 3 displays parameters of gyroscopic system.

A complete model is built by adding Eq.(6) to AUV model, enclosed with a structurally clear sketch in Figure 5.

PTO, generally acted as a spring damper system, offers damping and stiffness coefficients to gyro system. It could be expressed as:

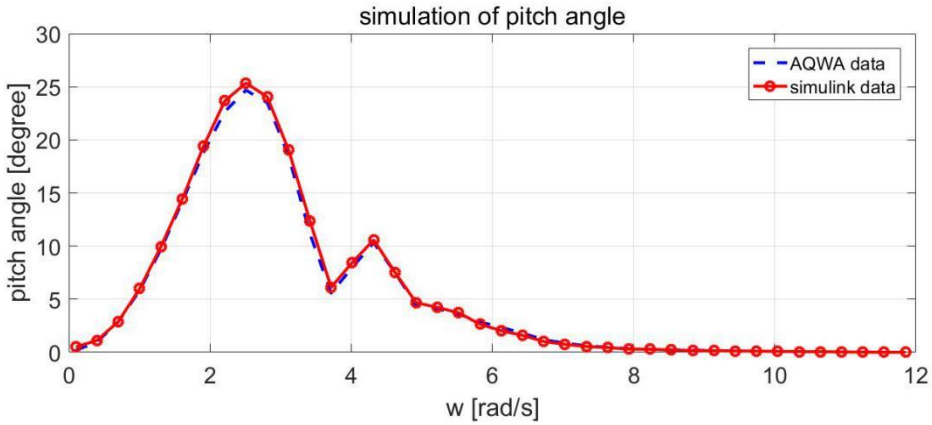

Figure 4. Simulation result of pitch motion

$$T_z = -k\varphi - c\dot{\varphi} \tag{20}$$

That is, PTO extracts active power through damper when precession φ oscillates. From the perspective of control theory, Eq.(20) makes up of a feedback loop of system, furthermore, plays a role of PD controller to the system. The Simulink model is shown in Figure 5.

By adding Eq.(20) to Eq.(6), neglecting the cosine term:

$$I_Z \ddot{\varphi} + c\dot{\varphi} + k\varphi = I_y \dot{\psi}\dot{\beta} \tag{21}$$

Eq. (21) expresses the linearized formula of the system around the axis of the PTO. The gyroscopic system is therefore equivalent to a second order LTI system. The active power P_d extracted from the damper[14]:

$$P_d = \frac{c}{2} w\varphi^2 = \frac{c}{2} \frac{\left(I_y \dot{\psi} j w \beta\right)^2}{I_y^2 \left[\left(w_n^2 - w^2\right)^2\right] + c^2 w^2} \tag{22}$$

w_n is defined as the natural frequency : $w_n = \sqrt{k / I_y}$. It is obvious the maximum power is absorbed when the system is resonating:

$$P_{d,max} = \frac{1}{2} \frac{\left(I_y \dot{\psi} w \beta\right)^2}{c} \tag{23}$$

Figure 6 shows that the linearized model gives an acceptable approximation of the full non-linear equations when the system is working at a certain condition.

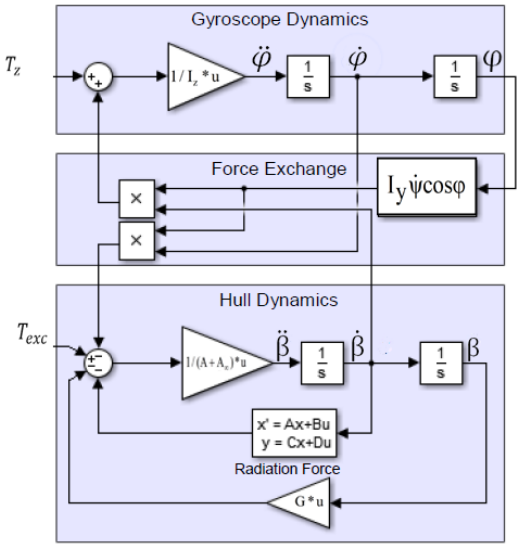

Figure 5. Simulation model of the system

With an input wave excitation moment connected to 1m wave height expressed as : $\tau_{exc} = 9434\sin(4.31t)$, k set as resonating condition, the precession axis oscillates approximately 72.7°around z-axis, and it provides a max active power at 3085W, of which rms is 1300W at the same time. The pitch angle declines from 10.63°(without adding gyro system) to 6.65°. It is a promising result as the gyro system at a certain realistic condition provides considerable active power.

Eq.(23) indicates the parameters that influence the extracted power consists of PTO stiffness, PTO damper, flywheel speed and wave frequency. A series of scattering graphs representing the power extracted with respect to the PTO damping coefficient and the gyro angular speed is shown in Figure 7. Four frequency points, in the range of 1-6 rad/s, the mainly frequency range of ocean wave, are selected. The PTO stiffness coefficient is tuned in accordance with resonating condition.

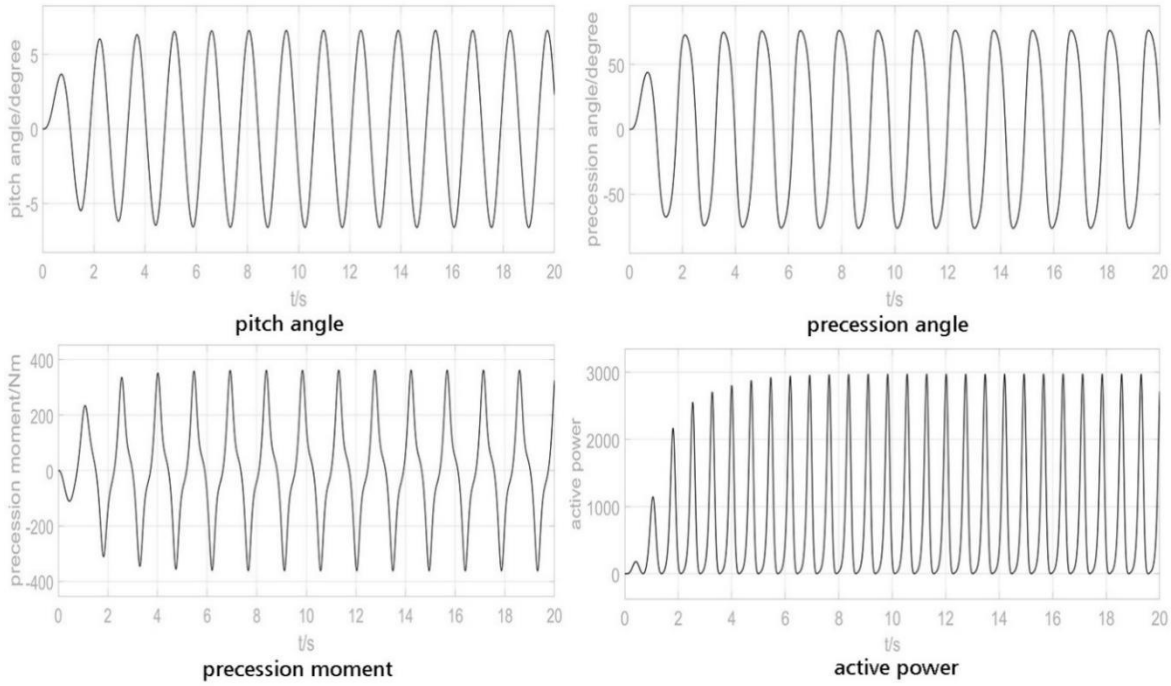

Figure 6. Simulation result of AUV system with k=57.02,c=40 and $\dot{\psi}$ =2400rpm.

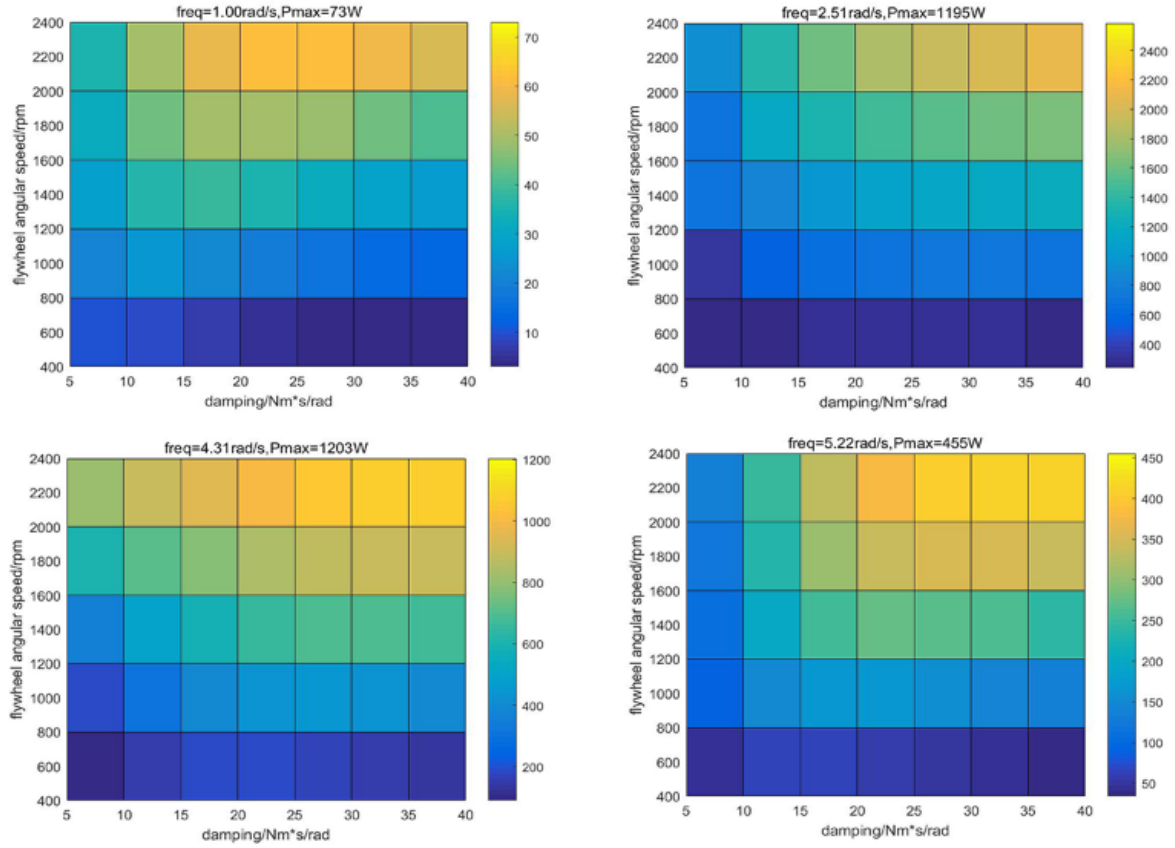

Figure 7. Power capabilities of gyroscopic system

How each parameter influences power extraction is summarized as follows: PTO stiffness is designed to match the resonating condition. Moreover, the more the stiffness changes from the wave resonant value, the smaller is the power absorbed by the damper. Both plots of Figure 7 indicates an optimal option exists for the damping coefficient, but if c is not at its optimal value, the power drops dramatically. The flywheel angular speed is another important parameter. As is shown above, the faster it is, the more power it is obtained. But it should be noticed that raising too much the gyro speed, makes the torque on the float to increase, and the gyroscopic system behaves as a float stabilizer but it is unsuitable for power generation. Finally, wave frequency decides the extracted power level, because the frequency-depended pitch motion gives the source of power.

Given a normal one or two class sea state, wave condition could be considered as superposition of a range of random sinusoidal wave of different frequency from 0.3~3 rad/s, the first, third and fourth plot of Figure 7 represents the most common result of power extraction, Pmax is obtained under optimal condition, while the second plot represents theoretical maximum value of active power. We could come to conclusion that the generated power is sufficient to provide power for a range of sensors (see Table 4)

It is an encouraging result, however, for optimal power the system needs to be adequately matched to the vehicle. From the results and this understanding, practically the system may be particularly suited for coastal water (limited fetch) applications, where the waves are typically fragmentized in frequency (compared to ocean swell) and where greater the irregularity of vehicle pitch motions, which might leads to the true result away from the simulation result[15].

The further study should be focused on the control design under irregular wave excitation moment, a condition more close to the true ocean wave state. The author will also endeavour to upgrade algorithm to make the result more practical.

Table 4. Typical power consumption of various AUV sensors

AUV particulars	Basis
Pressure sensor	0.1 (typ)
Digital compass	0.132 (typ) 0.014 (sleep)
Sound velocity sensor	0.25 (typ)
Echo sounder	0.25 (max)
Fluorometer	0.3 (typ)
Precision timing reference	0.3 (max)
Hydrophone	0.12–0.3 (typ)
MEMS AHRS and GPS/INS	0.675–0.95 (typ)
Turbulence sensor	1 (typ)
2D imaging sonar	3 (typ)
Conductivity temperature depth (CTD) sensor	3.42 (incl. pump)
Digital camera	5 (typ)
Sidescan sonar	5 (typ exclude CPU)
Nitrate sensor	7.5 (max)
Doppler velocity log	12 (max transmit) 2 (average transmit) 1.1(typ)
3D imaging sonar	15 (typ)
Underwater RF	16 (transmit) 5 (receive) 0.005 (sleep)
Current profiler	20–0.3 (transmit) 0.2–1.4 (typ)
Side scan sonar and sub bottom profiler	30 (max)
Navigation and control system	50 (max) 2 (active listening) 0.7 (sleep)
Multibeam swath bathymetry and sidescan	50 (max) 20 (standby)
Transponder	50 (max) 2 (active) 0.7 (sleep)
Underwater laser scanner	144 (typ)

5. Conclusion

This paper proposes a gyroscopic system to recharge an autonomous underwater vehicle (AUV) by using wave energy. A theoretical description of the whole system is provided including derivations of the governing equations of gyroscopic motion (a momentum function around precession axis is highlighted) and hydrodynamic equation of AUV. the active power is obtained through PTO damper, by form of product of damping coefficient and precession angular speed. Simulation results for a pitching AUV is given including the pitch angle, precession torque, precession angle and active power. To maximize the active power, a PD controller is conducted. The control design is summarized in section 4.Four factors: PTO stiffness coefficient, PTO damping coefficient, flywheel angular speed and wave frequency jointly affected the results. In a word, the extracted power reaches its peak under resonating condition. Simulation result is presented with input of sinusoidal excitation moment matched to 1 m wave height. By comparing the electrical power the AUV sensor required with the mechanical power provided by the gyro system, we reach a preliminary conclusion that this gyroscopic system could offer sufficient power to AUV. Finally, the author proposes the future research direction: focusing on the power performance under the irregular wave condition, by means of designing a more intelligent algorithm to achieve optimal or suboptimal control.

References

[1] Hongwei Fang, Ya Chen, Xiaoli Hu 2015 Wave Power Generation System and Its Control *J.Journal of Shenyang University (Natural Science Edition)*.**27**(5):376-384.

[2] Raffero M , Cagninei A and Giorcelli E 2013 Control and productivity analysis of the full scale ISWEC prototype *C.International Conference on Clean Electrical Power. IEEE*. Alghero, Italy.

[3] Hunt, J 2013 Global Inventory of AUV and Glider Technology available for Routine Marine Surveying. *Southampton UK for NERC Marine Renewable Energy Knowledge Exchange* pp 147-153.
[4] Chengliang Sun, Jiangbin Zhao and TianYu Cui 2017 Application Status and Prospect of AUV Power Battery Technology *J. Ship engineering*.**07**:69-74.
[5] Crimmins D M , Patty C T and Beliard M A 2006 Long-endurance test results of the solar-powered AUV system *C. Oceans. IEEE*. Boston, MA, USA.
[6] Townsend N and Shenoi A 2014 Recharging autonomous underwater vehicles from ambient wave induced motions *C.Oceans. IEEE*. Monterey, America.
[7] Townsend N C and Shenoi R A 2016 Feasibility study of a new energy scavenging system for an autonomous underwater vehicle *J. Autonomous Robots*. **40**(6):973-985.
[8] Cummins W E 1962 The impulse response function and ship motions *J. Schiffstechnik*.**9**:101-109.
[9] Jianping Chen, Hu Lei and Weiwei Tang 2017 *Ship Theory*(Harbin: Harbin Engineering University Press).
[10] Newman J 1977. *Marine Hydrodynamics*(Massachusetts–MITPress).
[11] Duarte, Sarmento and Alves 2013 State-Space Realization of the Wave-Radiation Force within FAST *J. Office of Scientific & Technical Information Technical Reports*. **20**(14):V008T09A021-V008T09A021.
[12] Perez T and Fossen T I 2011 Practical aspects of frequency-domain identification of dynamic models of marine structures from hydrodynamic data *J. Ocean Engineering*. **38**(2):426-435.
[13] McPhail and Stephen 2009 Autosub6000:A deep diving long range AUV *J. Journal of Bionic Engineering*. **6**(1):55–62.
[14] Bracco G , Giorcelli E and Mattiazzo G 2011 ISWEC: A gyroscopic mechanism for wave power exploitation *J. Mechanism & Machine Theory*. **46**(10):1411-1424.
[15] Novo R, Bracco G, Sirigu SA, Mattiazzo G, Mérigaud A and Ringwood JV 2018 Non Linear Simulation of a Wave Energy Converter With Multiple Degrees of Freedom Using a Harmonic Balance Method *C. ASME. International Conference on Offshore Mechanics and Arctic Engineering*. Volume **10**: Ocean Renewable Energy